Inorganica Chimica Acta 388 (2012) 16–21

Contents lists available at SciVerse ScienceDirect

Inorganica Chimica Acta

journal homepage: www.elsevier.com/locate/ica

Structures and luminescent properties of Tb(III) and Tb(III)–Ni(II) coordination polymers based on pyridyl dicarboxylate

Jing Huang [a,b], Hongmiao Li [a], Jianyong Zhang [a,*], Long Jiang [a], Cheng-Yong Su [a]

[a] KLGHEI of Environment and Energy Chemistry, School of Chemistry and Chemical Engineering, Sun Yat-Sen University, Guangzhou 510275, China
[b] Environmental Energy and Materials Laboratory, Guangzhou Institute of Energy Conversion, Chinese Academy of Sciences, No. 2, Nengyuan Rd., Wushan, Tianhe District, Guangzhou 510640, China

ARTICLE INFO

Article history:
Received 12 June 2010
Received in revised form 26 February 2012
Accepted 1 March 2012
Available online 10 March 2012

Keywords:
Coordination polymers
N,O ligands
Heterometallic complexes
Crystal structures
Luminescence

ABSTRACT

The N,O ligand, namely 5-(pyridin-4-yl)isophthalic acid (LH_2), with carboxylic acid groups and pyridyl group separated, prefers to act as a bridging ligand. Its Tb(III) coordination polymer, $[TbL(LH)(H_2O)_2]_\infty \cdot xH_2O$ (**1**), and heterometallic Tb(III)–Ni(II) coordination polymer, $[TbNiL_2(LH)(H_2O)]_\infty \cdot xH_2O$ (**2**), have been successfully prepared. Complex **1** exhibits a two-dimensional layered structure with (4,4) network leaving all the pyridyl N-donors uncoordinated, while complex **2** has a three-dimensional structure due to coordination of Ni(II) to part of pyridyl N-donors. Both the complexes were characterized by single-crystal X-ray diffraction, X-ray powder diffraction, FT-IR spectroscopy and thermogravimetry analysis. The ligand is capable of sensitizing the Tb(III) ion, and both the complexes emit characteristic visible green luminescence of Tb(III).

1. Introduction

Lanthanide-based coordination polymers are attracting increasing attention due to their interesting photophysical properties, arising from f–f transitions generated via the "antenna effect" [1–3]. In these complexes, the organic ligand can efficiently absorb energy and transfer it to the metal ion so that they exhibit sharp-emission luminescence properties and long luminescence lifetimes [4–8]. Heterometallic assemblies are interesting because the properties of one metal ion may be controlled by tuning the physicochemical properties of the other ion [9,10]. Hard–soft acid–base (HSAB) distinctions can be employed to construct heterometallic assemblies [11–13]. In this regard, pyridyl carboxylic acids are extensively explored to build heterometallic coordination polymers [14–21], because the lanthanide and transition metal ions have different affinities for the N- and O-donors [1,2,22]. Harder Ln(III) ions tend to bind to harder functional groups (carboxylates) preferentially over softer N-containing pyridyl groups. The second transition metal ion may provide an additional building unit to construct different structures on one hand. On the other hand, the introduction of the second metal ion may influence the luminescence.

Recently heterometallic coordination polymers of Ln(III)-d^{10} close-shell transition metal ions such as Zn(II) [23], Cd(II) [24,25], Ag(I) [26–29], Cu(I) [30] ions have been intensively studied. These metal ions have filled core-like d-orbitals and no d–d transitions are possible. In contrast, the introduction of open-shell ions may change the luminescent properties of coordination polymers, for example, Cu(II) has been shown to provide an alternate pathway for energy dissipation [31,32]. We notice that luminescent properties have been little studied for the latter group of heterometallic coordination polymers, even if some heterometallic coordination polymers were reported for study of their magnetic properties, for example, Ln(III)–Ni(II) coordination polymers [33–37]. In this paper, two Tb(III) coordination polymers are reported based on 5-(pyridin-4-yl)isophthalic acid (LH_2) with N- and O-donors, and incorporation of Ni(II) is found to cause changes of the photoluminescent properties.

2. Experimental

2.1. Materials and methods

All chemicals and solvents used were of reagent grade and used without further purification. Infrared spectra were measured on a Nicolet Avatar 330 FT-IR spectrometer with KBr pellets. X-ray powder diffraction data was recorded on a Bruker D8 Advance diffractometer at 40 kV, 40 mA with a Cu-target tube and a graphite monochromator. Thermogravimetric analysis (TGA) was performed in air and under 1 atm. of pressure at a heating rate of 10 °C/min on a NETZSCH Thermo Microbalance TG 209 F3 Tarsus.

* Corresponding author. Tel.: +86 20 8411 0539; fax: +86 20 8411 5178.
E-mail address: zhjyong@mail.sysu.edu.cn (J. Zhang).

0020-1693/$ - see front matter © 2012 Elsevier B.V. All rights reserved.
http://dx.doi.org/10.1016/j.ica.2012.03.004

UV–Vis absorption and luminescence spectra for the solid samples were recorded on a UV-3150 UV–Vis spectrophotometer (Shimadzu) and a Lifetime and Steady State Fluorometer FLS920 Combined Fluorescence Lifetime and Steady State Spectrometer (Edinburgh Instruments Ltd.), respectively.

2.2. Synthesis of 5-(pyridin-4-yl)isophthalic acid (LH_2)

$KMnO_4$ (5.8 g) in H_2O (10 mL) was added in a number of portions at 80 °C during a period of around 1 week to a solution of 4-(3,5-dimethylphenyl)pyridine [38] (0.75 g, 4.1 mmol) in H_2O/*t*-BuOH (v:v = 1:1, 20 mL) until the purple color of $KMnO_4$ did not fade after the last charge. The hot mixture was filtered to remove insoluble solids, and a solution of $Na_2S_2O_3$ (ca. 2 mol L^{-1}) was then added into the solution until the purple color disappeared. The solution was acidified by H_2SO_4 (1 mol L^{-1}) to pH ≈ 5. The white precipitate was filtered and dried (0.72 g, 72%) [39].

2.3. Synthesis of $[TbL(LH)(H_2O)_2]_\infty \cdot xH_2O$ (**1**)

A mixture of LH_2 (48.6 mg, 0.2 mmol), $TbCl_3$ (26.5 mg, 0.1 mmol), Et_3N (40.5 mg, 0.4 mmol) and H_2O (5 mL) was placed in a Teflon-lined autoclave and heated statically at 140 °C for 4 days under autogeneous pressure. After the reactant mixture was slowly cooled down to room temperature, the aqueous supernatant was decanted and the product was repeatedly washed with water and then left to dry at room temperature. Pale yellow block crystals of **1** were obtained, yield: 20.4 mg (29% based on Tb). Elemental *Anal.* Calc. for $TbC_{26}H_{19}N_2O_{10}\cdot H_2O$ (696.384): C, 44.84; H, 3.04; N, 4.02. Found: C, 44.60; H, 3.32; N, 3.96%. IR (cm^{-1}, KBr): 3390 br, 1612 s, 1550 s, 1517 sh, 1451 s, 1380 s, 1300 m, 1280 m, 1242 w, 1168 w, 1104 w, 1070 w, 939 w, 873 w, 839 w, 775 m, 737 m, 721 sh, 633 m, 610 w, 578 w.

2.4. Synthesis of $[TbNiL_2(LH)(H_2O)]_\infty \cdot xH_2O$ (**2**)

The synthesis was similar to that described for **1**. A mixture of LH_2 (48.6 mg, 0.2 mmol), $TbCl_3$ (26.5 mg, 0.1 mmol), $Ni(OAc)_2\cdot 4H_2O$ (12.4 mg, 0.05 mmol), Et_3N (40.5 mg, 0.4 mmol) and H_2O (5 mL) was heated at 140 °C for 4 days. After the reactant mixture was slowly cooled down to room temperature, two types of crystals were obtained and separated manually in the aid of microscope, pale yellow crystals of **1** (yield: 5.4 mg, 8% based on Tb) and green lamellar crystals of **2** (yield: 23 mg, 24% based on Tb). Elemental *Anal.* Calc. for $TbNiC_{39}H_{24}N_3O_{13}\cdot 2H_2O$ (996.297): C, 47.02; H, 2.83; N, 4.22. Found: C, 47.35; H, 3.20; N, 4.28%. IR (cm^{-1}, KBr): 3381 br, 1620 s, 1580 s, 1509 m, 1445 m, 1414 m, 1380 s, 1300 m, 1230 w, 1208 w, 1177 w, 1107 w, 1080 w, 873 w, 837 m, 777 m, 741 sh, 719 m, 646 m, 610 w, 579 w, 548 w, 507 w.

2.5. X-ray structure analyses

The intensity data were collected using a Bruker Smart 1000 CCD diffractometer with graphite monochromated Cu Kα (λ = 1.54178 Å) radiation for **1** or and an Oxford Gemini S Ultra diffractometer equipped with graphite monochromated Enhance (Mo) X-ray source (λ = 0.71073 Å) for **2**. The structures were solved by the direct methods following difference Fourier syntheses, and refined by the full-matrix least-squares method against F_0^2 using SHELXTL software [40]. All non-hydrogen atoms except those displaying severe disorder were refined with anisotropic thermal parameters while hydrogen atoms were introduced in the final refinement model in calculated positions with isotropic thermal parameters. In case of disorder, appropriate restraints were applied to model the molecules to the idealized geometry. Crystallographic data for complexes **1** and **2** are summarized in Table 1.

Table 1
Crystallographic data for **1** and **2**.

	1	**2**
Empirical formula	$C_{52}H_{40}N_4O_{21}Tb_2$	$C_{78}H_{54}N_6O_{29}Ni_2Tb_2$
FW	1374.72	1974.53
Crystal system	orthorhombic	monoclinic
Space group	*Pba*2	$P2_1/c$
a (Å)	31.7963(4)	11.3219(2)
b (Å)	7.4231(1)	24.0980(4)
c (Å)	9.8644(1)	14.0045(2)
α (°)	90	90
β (°)	90	104.1461(18)
γ (°)	90	90
V (Å^3)	2328.27(5)	3705.04(16)
Z	2	4
ρ_{calc} (g cm^{-3})	1.961	1.770
μ (mm^{-1})	15.563	2.479
T (K)	150(2)	150(2)
GOF	1.053	0.962
R_{int}	0.0497	0.0518
R_1 [$I > 2\sigma(I)$]	0.0512	0.0454
wR_2 [$I > 2\sigma(I)$]	0.1368	0.1046

3. Results and discussion

3.1. Design and syntheses

5-(Pyridin-4-yl)isophthalic acid (LH_2) is a bridging ligand with two carboxylic acid groups and one pyridyl group. The ligand was chosen because that lanthanide ions (e.g. Tb(III)) are preferably sequestrated by the carboxylate group, and borderline transition metal ions (e.g. Ni(II)) may have the dual affinity for either the carboxylate group or the pyridyl group according to the HSAB matching [41]. In addition, the carboxylic acid groups and the pyridyl groups are separated further in LH_2 in comparison with previously reported pyridyl carboxylic acids [1,2,22], thus the ligand prefers to act as a bridging ligand as opposed to a chelating ligand. Solvothermal reaction of LH_2, $TbCl_3$ and Et_3N in H_2O at 140 °C for 4 days resulted in the formation of pale yellow crystals of **1**. When the reaction was performed in the presence of $Ni(OAc)_2\cdot 4H_2O$, pale yellow crystals of **1** and green crystals of **2** were obtained as a mixture, which could be separated manually in the aid of microscope. Their formula of $[TbL(LH)(H_2O)_2]_\infty \cdot xH_2O$ (**1**) and $[TbNiL_2(LH)(H_2O)]_\infty \cdot xH_2O$ (**2**) were further confirmed by elemental analysis and thermal gravimetric analysis (TGA).

3.2. Crystal structures

Single crystal X-ray diffraction analysis shows that $[TbL(LH)(H_2O)_2]_\infty \cdot xH_2O$ (**1**) crystallizes in the orthorhombic space group *Pba*2. The asymmetric unit contains one Tb(III) ion, two ligands and two coordinated water molecules. The Tb(III) ion is nine-coordinated by seven oxygen atoms from four ligands and two oxygen atoms from two coordinated water molecules (Fig. 1a). All the pyridyl N donors of the ligands do not bind to Tb(III) ion, therefore each ligand bridges two metal ions, yielding an undulating 2D layer with a (4,4) network if the ligand is simplified as a 2-connecting node (Fig. 1b–d). The coordination modes of LH_2 are summarized in Scheme 1. There are two types of ligands (Type A and B) linking every two Tb(III) ions in **1**. For the ligand of type A, one carboxylate group connects with one Tb atom through a monodentate O atom in a η^1-mode and the other carboxylate group binds to a second Tb atom through both carboxylate oxygens in a η^2-mode. Two ligands of type A bind to one Tb(III)

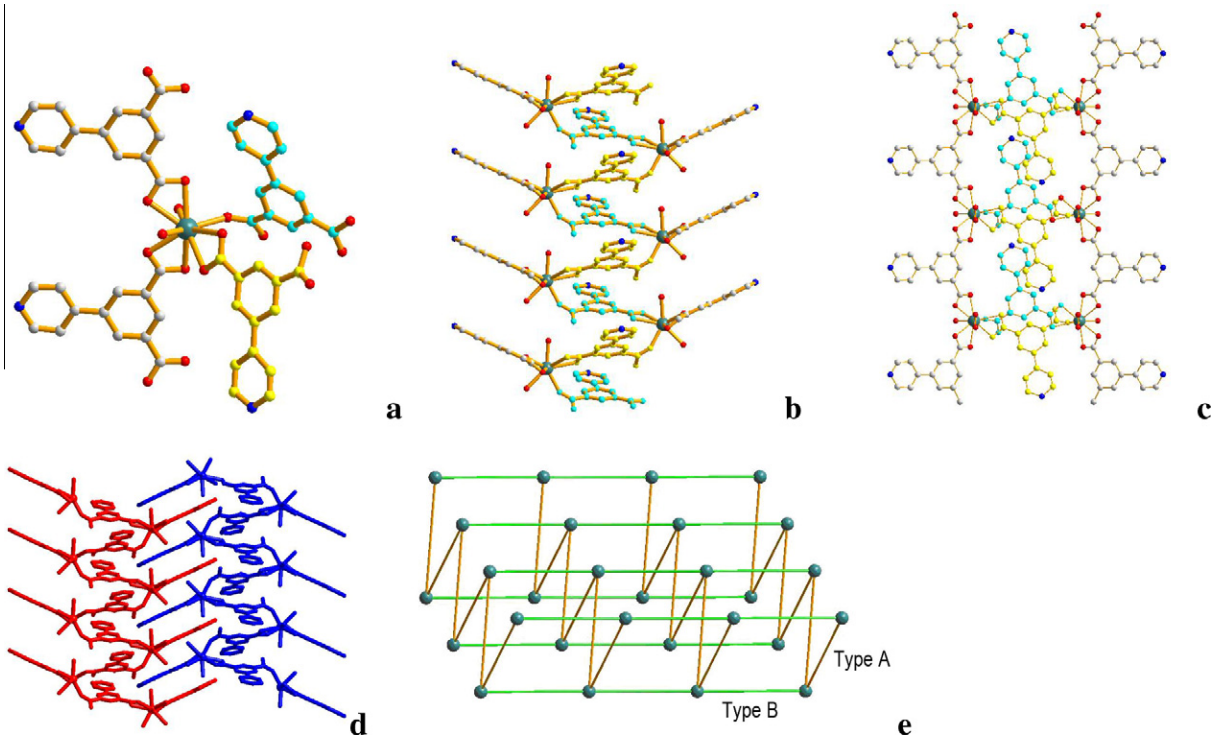

Fig. 1. (a) The coordination environment around the Tb(III) ion with hydrogen atoms and guest water molecules omitted, part of the 2D layer viewed along (b) *c*-axis and (c) *b*-axis, (d) two adjacent layers and (e) a (4,4) topological diagram of **1**.

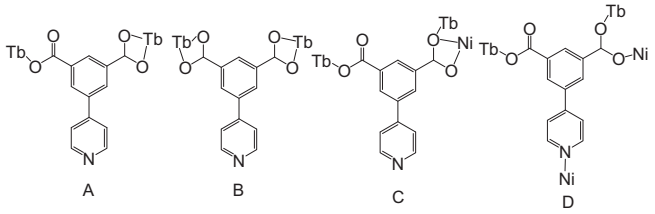

Scheme 1. Coordination modes of 5-(pyridin-4-yl)isophthalic acid (LH_2) in **1** (A and B) and **2** (C and D).

ion with the angle Tb···Tb···Tb of 41.63°, which results in the undulating shape of the 2D layer (Fig. 1e). The pyridyl groups of type A are protonated, which is confirmed by the charge balance and bond valence sum calculations. Intralayer hydrogen bonding exists between the protonated pyridyl group and the carboxylate O atom (N–H···O 2.752(10) Å, ∠N–H···O 164.2°). For the ligand of type B, both the carboxylate groups bind to Tb in a η^2-mode. The ligands of type B bind to Tb(III) ion in straight line (Fig. 1e). Due to the different coordination modes, the distances of Tb···Tb are slightly different, i.e. 10.444 Å bridged by the type A ligands and 9.864 Å bridged by the type B ligands. The undulating 2D layers are stacked in a gearing mode via offset-face-to-face π–π interaction between the pyridyl ring and the phenyl ring with interplanar distance ca. 3.45 Å, and hydrogen bonding between the coordinated water molecules and the carboxylate O atoms. The network accommodates solvated water molecules as guests between the layers.

X-ray structure determination was performed to reveal that $[TbNiL_2(LH)(H_2O)]_\infty \cdot xH_2O$ (**2**) crystallizes in the monoclinic space group $P2_1/c$. The asymmetric unit contains one Tb(III) ion, one Ni(II) ion, three ligands and one coordinated water molecules (Fig. 2a), with C and O atoms of one carboxylate group disordered crystallographically at two positions. Ni(II) is six-coordinated and has a distorted octahedral geometry with a N2O4 donor set. The N2O4 donor set is supplied by two pyridyl N donors and four carboxylate O donors from five different ligands, among which one carboxylate group links to the Ni atom in bidentate-chelate mode. Tb(III) is seven-coordinated with a pentagonal bipyramid coordination geometry. The seven coordination sites are occupied by six O atoms from six different ligands and one coordinated water molecule. Adjacent Tb(III) and Ni(II) ions are triply bridged into a TbNi heterometallic binuclear building unit by one bidentate bridging carboxylate group and two bridging carboxylate groups with the Tb···Ni distance of 3.926 Å. Totally eight ligands are coordinated to the TbNi unit (Fig. 2b and c). Four TbNi heterometallic units are connected to a quadrangle (Fig. 2d). Every two TbNi units are doubly bridged by two ligands, and the connectivities of four edges are different from each other. For the first edge with Tb···Tb distance of 9.75 Å (green[1], Fig. 2d), two TbNi units are bridged by two ligands with both the pyridyl N-donors uncoordinated. The uncoordinated pyridyl groups are protonated, which is confirmed by the charge balance and bond valence sum calculations. H-bond exists between pyridyl N–H and neighboring carboxylate O atom with N···O separation of 2.637 Å and N–H···O angle of 144.7°. For the other three edges with Tb···Tb distances of 10.48, 10.53, 10.53 Å, respectively (pink, dark red and pale blue, Fig 2d), the pyridyl N-donor of all the five ligands are coordinated. Three of the five ligands are shared by other edges in the same or different quadrangles, and thus the quadrangles formed by four TbNi units are extended to form a waving 2D layer (Fig. 2e). The remaining two of the ligands (in the dark red and pale blue edges) have the pyridyl N-donors available as pillars to support the adjacent layers into 3D supramolecular architecture by coordinating with Ni atoms located in the adjacent layer (Fig. 2f). The 3D network accommodates solvated water molecules as guests in the pillared

[1] For interpretation of color in Fig. 2, the reader is referred to the web version of this article.

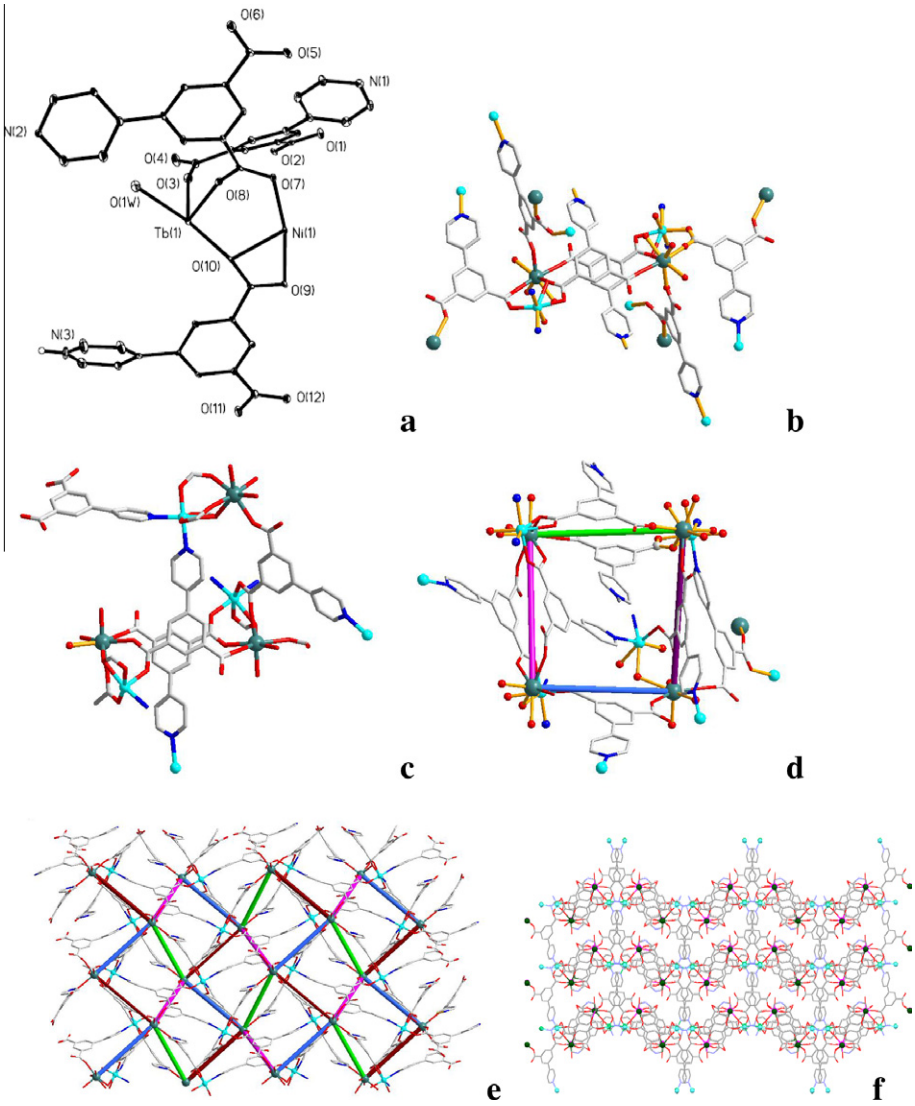

Fig. 2. (a) ORTEP diagram showing the asymmetric unit of **2** with hydrogen atoms and guest water molecules omitted (thermal ellipsoids with 30% probability); (b and c) connectivity of two neighboring TbNi units; (d) a quadrangle formed by four TbNi units; (e) a [1 0 0] layer; (f) two layers packing along the *a*-axis. For clarity, only one position was kept for the disordered C and O atoms.

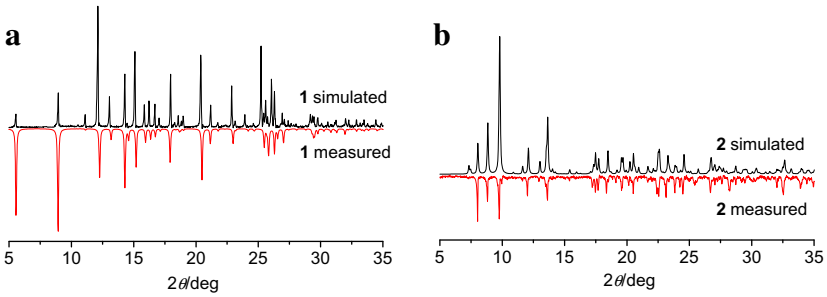

Fig. 3. X-ray powder diffraction patterns of **1** and **2** (simulated (top) and measured (below)).

space. The net topological analysis of complex **2** reveals a 3-nodal (3,7)-connected net with stoichiometry $(3\text{-c})_2(7\text{-c})$ if the TbNi heterometallic units are considered as nodes. The point (Schläfli) symbol for **1** is $(4{\cdot}6^2)(4^2{\cdot}5)(4^3{\cdot}5^5{\cdot}6^8{\cdot}7^3{\cdot}8^2)$ calculated with TOPOS [42].

In complex **2**, the ligand adopts two coordination modes different from those in complex **1**. One ligand acts as a tri-connector (Type C, Scheme 1) to link two Tb atoms and one Ni atoms. One carboxylate group is linked to Tb though monodentate carboxylic O atoms, the other carboxylate group bridges Tb and Ni in a bridging-chelating mode, and the pyridyl N atom is uncoordinated. The other ligand acts as tetra-connector (Type D, Scheme 1). One carboxylate group bridges Tb and Ni atoms in a carboxylate O,O′ mode, the other links to another Tb atom in monodentate mode. The pyridyl N atom bonds to the second Ni center.

The structures of **1** and **2** reveals that Tb(III) is exclusively sequestrated by oxygen and borderline Ni(II) has the dual affinity for N

and O-donors, which is consistent with the HSAB matching as expected [41]. All the pyridyl N-donors are uncoordinated in **1**, while part of the N-donors are coordinated to Ni(II) ions in **2**.

Pure sample of **1** was obtained, and that of **2** could be separated manually from the mixed phase. X-ray powder diffraction patterns were recorded to check the solid-state phase purity of the bulky samples of complexes **1** and **2** (Fig. 3). The measured patterns are closely matching the theoretical ones, indicative of satisfactory solid-state phase purity.

3.3. Infrared spectroscopy

FT-IR spectrum of **1** shows two strong bands at 1612 and 1550 cm^{-1}, which are assigned to the asymmetric modes $\nu_{asym}(CO_2)$ and shifted to lower wavenumbers compared with the free ligand at 1699 cm^{-1}. The symmetric modes $\nu_{sym}(CO_2)$ give rise to the strong bands at 1451 and 1380 cm^{-1}. The IR spectrum of **2** is similar to that of **1**. The bands observed for **2** at 1620 and 1580 cm^{-1} are attributed to the asymmetric stretching vibrations of carboxylate groups, and those at 1445, 1414 and 1380 cm^{-1} are regarded as the symmetric stretching vibrations.

3.4. Thermogravimetric analysis

Thermogravimetric analysis was performed for **1** and **2** under air on crystalline samples to investigate the mobility of the solvated molecules (Fig. 4). Complex **1** shows a weight loss of 7.2% on heating from room temperature to 280 °C, which is attributed to the release of the solvated molecules, and the decomposition of the residue occurs above 390 °C. The TG curve of **2** shows gradual weight losses of solvated molecules of 11.2% before the decomposition of the framework at about 380 °C.

3.5. Photoluminescent properties

The solid-state UV–Vis spectra of the free ligand and complexes **1** and **2** are shown in Fig. 5. The ligand exhibits a broad absorption band with the maximum at 260 nm, corresponding to intraligand $n \rightarrow \pi^*$ and $\pi \rightarrow \pi^*$ transitions. The absorption spectrum for **1** shows a broad band with the maximum at 319 nm, which is red-shifted for 59 nm. Yet **2** shows the presence of additional bands centered at about 392 and 664 nm besides a similar band with

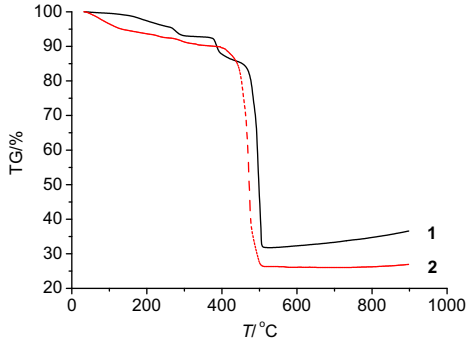

Fig. 4. TG curves for $[TbL(LH)\cdot 2H_2O]_\infty \cdot xH_2O$ (**1**) and $[TbNiL_2LH\cdot H_2O]_\infty \cdot xH_2O$ (**2**).

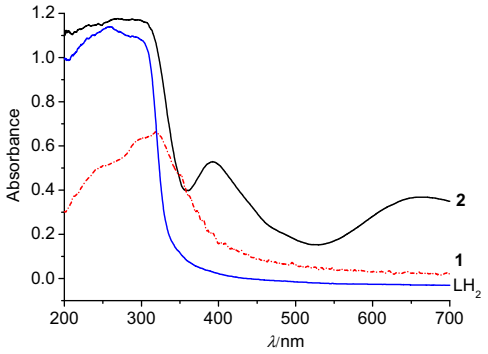

Fig. 5. Absorbance spectra of the free ligand LH_2, **1** and **2** in the solid state at room temperature.

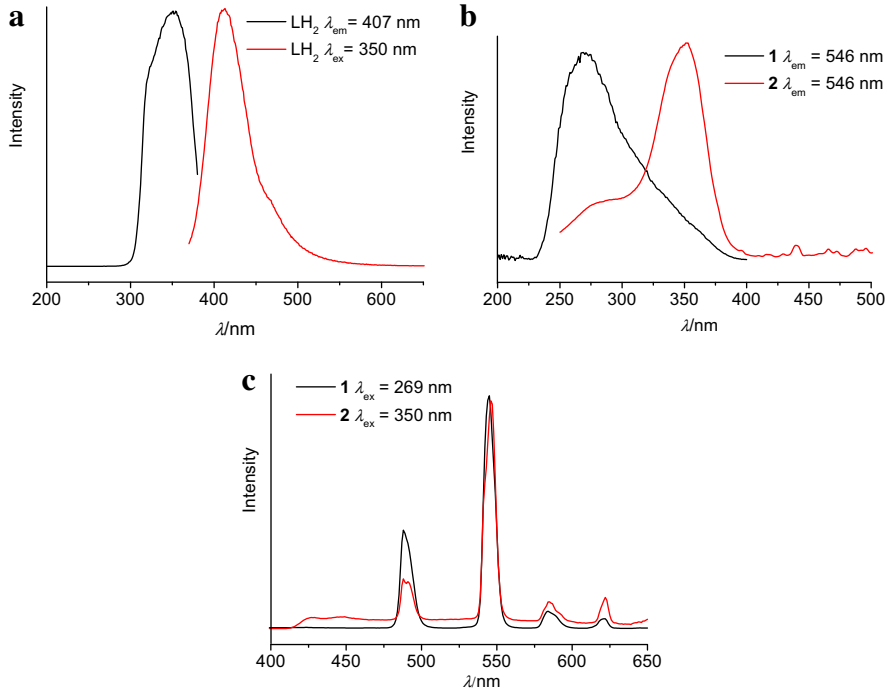

Fig. 6. Excitation and emission spectra of **1**, **2** and LH_2 in the solid state at room temperature.

the free ligand. The absorptions generated at 392 and 664 nm can be assigned to the $^3A_{2g} \rightarrow {}^3T_{1g}(P)$ and $^3A_{2g} \rightarrow {}^3T_{1g}(F)$, respectively, which are characteristic for Ni(II) in pseudo-octahedral geometry [43].

The free ligand presents an emission with the band peaking around 413 nm upon excitation at 350 nm (Fig. 6). Under UV excitation (λ_{ex} = 269 nm) complex **1** exhibits the characteristic visible emission peaks of Tb(III), and their four main emission peaks at 490, 545, 585 and 625 nm can be assigned to transitions from emitting level $^5D_4$ to the ground multiplet ^7F_n (n = 6, 5, 4, 3) of Tb(III) ion, respectively. The most intense emission is at 545 nm corresponding to $^5D_4 \rightarrow {}^7F_5$ transition. The excitation spectrum of **2** shows that a peak centered at around 350 nm turns distinct apart from the shoulder peak at 269 nm (Fig. 6). Excitation of **2** at 350 nm results in typical emission bands for the Tb(III) ion similar to those of **1**. These luminescent results suggest that metal emission was observed for both the complexes and the ligand (LH_2) can sensitize the luminescence of Tb(III) ions. Energy may be efficiently transferred from the excited states of the ligand to the excited states of the Tb(III) ions. The luminescent lifetimes (τ) were measured to show that the luminescence decay of **1** has an excited-state lifetime of 0.93(0.05) ms for $^5D_4 \rightarrow {}^7F_5$ transition (λ_{ex} = 269 nm), while the lifetime of the $^5D_4 \rightarrow {}^7F_5$ emission of **2** is decreased to 0.34(0.02) ms upon 350 nm excitation.

4. Conclusions

Based on a pyridyl dicarboxylic acid, 5-(pyridin-4-yl)isophthalic acid (LH_2), homometallic Tb(III) and heterometallic Tb(III)–Ni(II) coordination polymers have been prepared under hydrothermal conditions. The Tb(III)-only complex is a two-dimensional (4,4) network structure whereas the heterometallic complex is three-dimensional due to introducing of Ni(II). The ligand is capable of sensitizing the Tb(III) ion in both complexes, which emit characteristic green luminescence.

Acknowledgments

We are grateful to the NSFC (20903121), the NSF of Guangdong Province (S2011010001307), the RFDP of Higher Education of China, the Fundamental Research Funds for the Central Universities, and the SRF for ROCS of SEM for support.

Appendix A. Supplementary material

CCDC 773412 and 773413 contain the supplementary crystallographic data for complexes **1** and **2**, respectively. These data can be obtained free of charge from The Cambridge Crystallographic Data Centre via www.ccdc.cam.ac.uk/data_request/cif. Supplementary data associated with this article can be found, in the online version, at http://dx.doi.org/10.1016/j.ica.2012.03.004.

References

[1] M.D. Allendorf, C.A. Bauer, R.K. Bhakta, R.J.T. Houk, Chem. Soc. Rev. 38 (2009) 1330.
[2] C.L. Cahill, D.T. de Lilla, M. Frisch, CrystEngComm 9 (2007) 15.
[3] R.J. Hill, D.-L. Long, P. Hubberstey, M. Schröder, N.R. Champness, J. Solid State Chem. 178 (2005) 2414.
[4] C. Marchal, Y. Filinchuk, D. Imbert, J.-C.G. Bünzli, M. Mazzanti, Inorg. Chem. 46 (2007) 6242.
[5] G.F. Liu, Z.P. Qiao, H.Z. Wang, X.M. Chen, G. Yang, New J. Chem. 26 (2002) 791.
[6] X. Li, Y.B. Zhang, M. Shi, P.Z. Li, Inorg. Chem. Commun. 11 (2008) 869.
[7] X.P. Yang, R.A. Jones, J.H. Rivers, W.K. Wong, Dalton Trans. (2009) 10505.
[8] N. Sabbatini, M. Guardigli, J.-M. Lehn, Coord. Chem. Rev. 123 (1993) 201.
[9] S.V. Eliseeva, J.-C.G. Bünzli, Chem. Soc. Rev. 39 (2010) 189.
[10] J.-C.G. Bünzli, C. Piguet, Chem. Soc. Rev. 34 (2005) 1048.
[11] L.A. Gerrard, P.T. Wood, Chem. Commun. (2000) 2107.
[12] A.D. Burrows, M.F. Mahon, C.T.F. Wong, CrystEngComm 10 (2008) 487.
[13] J. Zhang, L.G. Hubert-Pfalzgraf, D. Luneau, Inorg. Chem. Commun. 7 (2004) 979.
[14] K.C. Szeto, K.O. Kongshaug, S. Jakobsen, M. Tilset, K.P. Lillerud, Dalton Trans. (2008) 2054.
[15] J. Hafizović, A. Krivokapić, K.C. Szeto, S. Jakobsen, K.P. Lillerud, U. Olsbye, M. Tilset, Cryst. Growth Des. 7 (2007) 2302.
[16] K.C. Szeto, C. Prestipino, C. Lamberti, A. Zecchina, S. Bordiga, M. Bjørgen, M. Tilset, K.P. Lillerud, Chem. Mater. 19 (2007) 211.
[17] K.C. Szeto, K.P. Lillerud, M. Tilset, M. Bjørgen, C. Prestipino, A. Zecchina, C. Lamberti, S. Bordiga, J. Phys. Chem. B 110 (2006) 21509.
[18] Y.G. Huang, M.Y. Wu, F.Y. Lian, F.L. Jiang, M.C. Hong, Inorg. Chem. Commun. 11 (2008) 840.
[19] Q. Yue, J. Yang, G.H. Li, G.D. Li, W. Xu, J.S. Chen, S.N. Wang, Inorg. Chem. 44 (2005) 5241.
[20] S. Noro, H. Miyasaka, S. Kitagawa, T. Wada, T. Okubo, M. Yamashita, T. Mitani, Inorg. Chem. 44 (2005) 133.
[21] M. Fang, B. Zhao, Y. Zuo, J. Chen, W. Shi, J. Liang, P. Cheng, Dalton Trans. (2009) 7765.
[22] W.S. Liu, T.Q. Jiao, Y.Z. Li, Q.Z. Liu, M.Y. Tan, H. Wang, L.F. Wang, J. Am. Chem. Soc. 126 (2004) 2280.
[23] Y.C. Liang, M.C. Hong, R. Cao, W.P. Su, Y.J. Zhao, J.B. Weng, R.G. Xiong, Bull. Chem. Soc. Jpn. 75 (2002) 1521.
[24] T. Gunnlaugsson, T.C. Lee, R. Parkesh, Org. Lett. 5 (2003) 4065.
[25] P. Jiang, L. Chen, J. Lin, Q. Liu, J. Ding, X. Gao, Z. Guo, Chem. Commun. 13 (2002) 1424.
[26] X.Q. Zhao, B. Zhao, W. Shi, P. Cheng, CrystEngComm 11 (2009) 1261.
[27] B. Zhao, X.Q. Zhao, Z. Chen, W. Shi, P. Cheng, S.P. Yan, D.Z. Liao, CrystEngComm 10 (2008) 1144.
[28] X.Q. Zhao, B. Zhao, S. Wei, P. Cheng, Inorg. Chem. 48 (2009) 11048.
[29] Y. Qiu, H. Liu, Y. Ling, H. Deng, R. Zeng, G. Zhou, M. Zeller, Inorg. Chem. Commun. 10 (2007) 1399.
[30] Q.B. Bo, Z.X. Sun, W. Forsling, CrystEngComm 10 (2008) 232.
[31] M. Frisch, C.L. Cahill, Dalton Trans. (2005) 1518.
[32] N.S. Gunning, C.L. Cahill, Dalton Trans. (2005) 2788.
[33] A.M. Madalan, K. Bernot, F. Pointillart, M. Andruh, A. Caneschi, Eur. J. Inorg. Chem. (2007) 5533.
[34] Z. He, C. He, E.Q. Gao, Z.M. Wang, X.F. Yang, C.S. Liao, C.H. Yan, Inorg. Chem. 42 (2003) 2206.
[35] T. Shiga, N. Ito, A. Hidaka, H. Ōkawa, S. Kitagawa, M. Ohba, Inorg. Chem. 46 (2007) 3492.
[36] T. Yamaguchi, Y. Sunatsuki, H. Ishida, M. Kojima, H. Akashi, N. Re, N. Matsumoto, A. Pochaba, J. Mrozinski, Bull. Chem. Soc. Jpn. 81 (2008) 598.
[37] C.A. Barta, S.R. Bayly, P.W. Read, B.O. Patrick, R.C. Thompson, C. Orvig, Inorg. Chem. 47 (2008) 2280.
[38] J. Huang, L. He, J. Zhang, L. Chen, C.Y. Su, J. Mol. Catal. A: Chem. 317 (2010) 97.
[39] S. Xiang, J. Huang, L. Li, J. Zhang, L. Jiang, X. Kuang, C.Y. Su, Inorg. Chem. 50 (2011) 1743.
[40] G.M. Sheldrick, SHELX-97: Program for Crystal Structure Solution and Refinement, University of Götingen, Götingen, Germany, 1997.
[41] R.G. Pearson, J. Am. Chem. Soc. 85 (1963) 3533.
[42] V.A. Blatov, M.V. Peskov, Acta Crystallogr., Sect. B: Struct. Sci. 62 (2006) 457.
[43] P.D. Bauer, M.S. Mashuta, R.J. O'Brien, J.F. Richardson, R.M. Buchanan, J. Coord. Chem. 57 (2004) 361.